Supporting Information

Dense Carbon Nanoflower Pellets for Methane Storage

Shucheng Chen[a], Huaxin Gong[a], Birol Dindoruk[b], Jiajun He[c,*] and Zhenan Bao[a,*]

[a]*Department of Chemical Engineering, Stanford University, Stanford, California, 94305, USA*
[b]*Shell International Exploration and Production Inc., Houston, USA*
[c]*Department of Mechanical Science and Engineering, University of Illinois at Urbana-Champaign , Urbana, IL, 61801, USA*

**Corresponding Authors: jiajunhe@illinois.edu, zbao@stanford.edu*

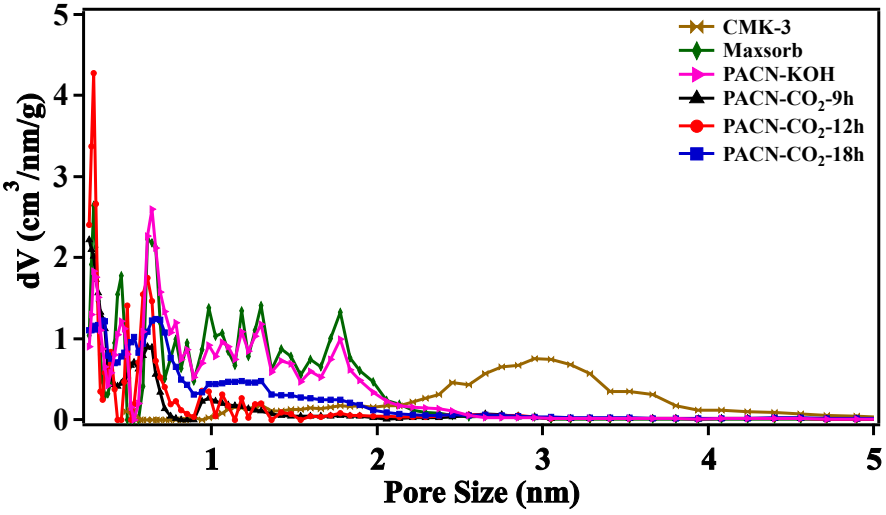

Figure S1. Pore size distributions for activated carbon flower particles and selected commercial carbon.

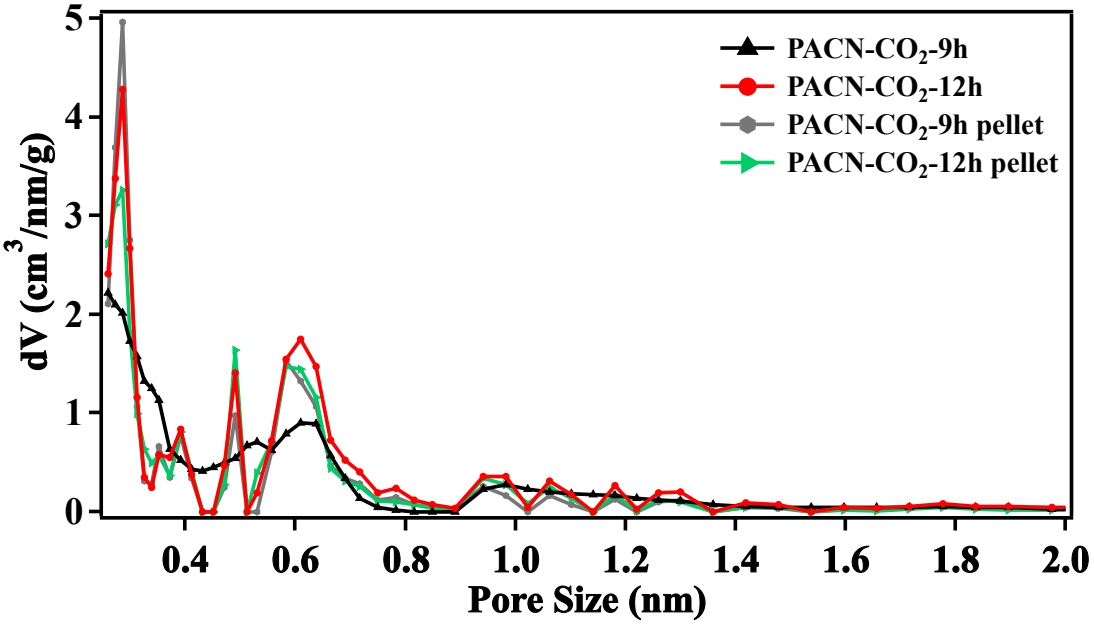

Figure S2. Pore size distributions for CO_2 activated carbon nanoflower pellets vs. powders.

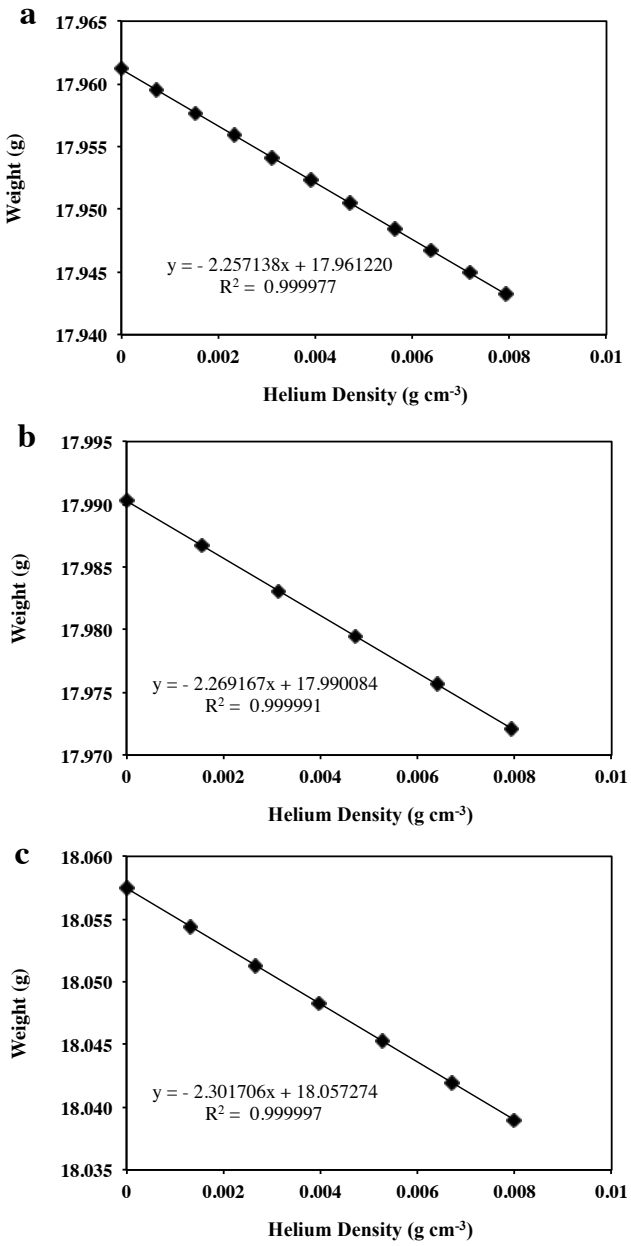

Figure S3. Helium buoyancy data at 100 °C for (a) empty basket; (b) basket with PACN-CO_2-9h pellet; and (c) basket with PACN-CO_2-12h pellet. The true mass and volume can be determined from the y-intercept and slope of the linear fit, respectively. The basket has a mass of 17.961220 g and a volume of 2.257138 cm^3, while the PACN-CO_2-9h pellet and -12h pellet samples have masses of 0.028864 g and 0.096054 g, and skeletal volumes of 0.012029 cm^3 and 0.044568 cm^3, respectively.

Table S1. Surface area, Pore Volume, Bulk Density, and Methane Storage Performance for Selected Promising Porous Materials at RT and 35 or 65 bar

Sample	S_{BET} (m^2/g)	Pore Volume (cm^3/g)	Bulk Density[a] (g/cm^3)	Literature Packing Density (g/cm^3)	Mass Storage (g/g) at 35 bar/65 bar	Volume Storage (cm^3/cm^3) at 35 bar/65 bar	Reference
monoHKUST-1	1193	0.56	1.06	-	0.149/0.177	224/259	**MOF [1]**
AX-21	4880	1.13	0.47	0.49	0.225/0.298	153/203	**Activated Carbon Materials [2,3]**
LMA405	3551	2.00	0.41	0.45	0.213/0.264	134/166	
LMA738	3290	2.25	0.36	0.53	0.222/0.296	165/220	
LMA726	3425	2.44	0.34	0.54	0.210/0.277	156/206	
CMK-3	936	1.18	0.54	-	0.111/0.149	83/111	**Tested Commercial Carbon**
Maxsorb	3270	1.71	0.44	-	0.148/0.198	111/150	
PACN-CO_2-9h	1143	0.77	0.75	-	0.124/0.146	131/154	**Carbon Flowers, Our Work**
PACN-CO_2-12h	1381	0.85	0.74	-	0.129/0.159	135/165	
PACN-CO_2-18h	1927	1.25	0.59	-	0.169/0.217	140/180	
PACN-KOH	3373	1.80	0.45	-	0.221/0.287	139/181	
PACN-CO_2-12h pellet	1188	0.67	0.87	-	0.135/0.161	165/196	
PACN-CO_2-9h pellet	1077	0.61	0.96	-	0.121/0.142	164/191	

[a]For the literature where the bulk density was not reported, the number listed in this table was calculated following the same equations and procedures described in this SI.

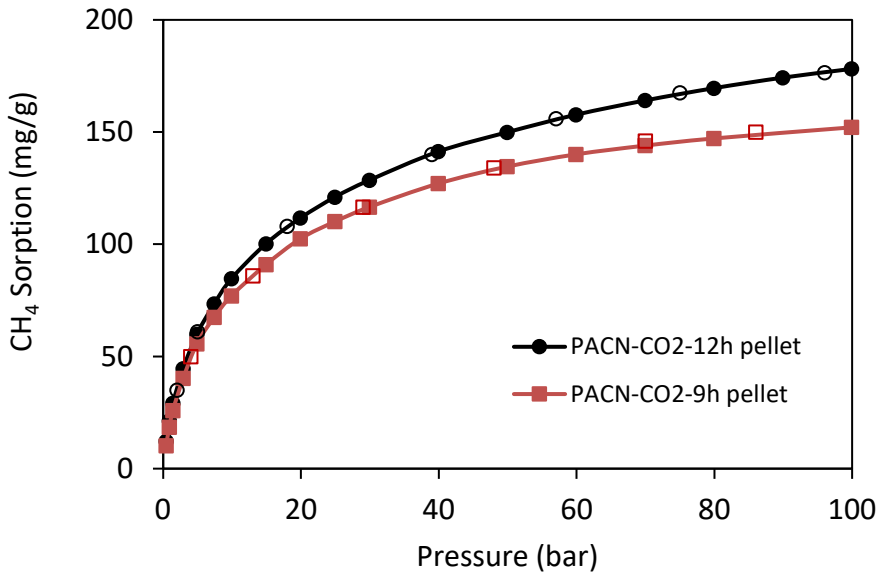

Figure S4. Methane adsorption (solid symbols) and desorption (hollow symbols) isotherms at 298 K for activated carbon nanoflower pellets.

Pore Volume Calculations

The selection of the relative pressure determines the upper limit of the pore size distribution to be included in the pore volume calculation. The upper limit of the pore size can be calculated using the Kelvin equation for a given adsorptive at a given temperature.[4] For example, the relative pressure of 0.9 allows nitrogen (77 K) to fill the pore up to a pore radius of

$$r = \frac{-2\gamma V_m}{RTln(p/p_0)} = \frac{-2(8.85)(34.6)}{(8.314 \times 10^7)(77)\ln(0.9)} = 9.08 \times 10^{-7}\ cm = 9.08\ nm$$

where γ (8.85 erg/cm^2) is the surface tension and V_m is the molar volume (34.6 cm^3/mol). This means that the pore volume estimated at the relative pressure of 0.9 is the total volume of all pores up to about 18 nm in diameter. In comparison, the pore volume calculated at the relative pressure of 0.995 corresponds to the total volume of all pores up to the size of 382 nm.

In a practical case, the macropores (> 50 nm) should be included in the pore volume estimation, since they exist as void space in the packed container. This will affect the subsequent volume-based methane adsorption calculations. Hence, a relative pressure of 0.995 is selected in the pore volume calculation.

Total and Excess Adsorption

Total adsorption is defined as the total amount of gas that resides within the adsorbent pore space at a given temperature and pressure, which represents the storage capacity in gas storage applications. Excess adsorption is defined as the difference in the amounts of total gas that resides in the unit pore volume and the bulk gas that has the same free volume at a given temperature and pressure. In a typical gravimetrical adsorption experiment, the excess adsorption is measured, while the total adsorption is estimated using the following equation:

$$n_{tot} = n_{ex} + \rho V_{pore}$$

where n_{tot} and n_{ex} stand for the total and excess adsorption, respectively. ρ represents the bulk density of free gas at the given temperature and pressure, which is obtained from the National Institute of Standards and Technology (NIST) chemistry webbook. V_{pore} is the total pore volume of the sorbent. In this work, the total pore volume is estimated from the nitrogen adsorption at 77 K and the relative pressure (p / p_0) of 0.995. Figure S4 illustrates the comparison of CH_4 total adsorption with excess adsorption for the PACN materials at 298 K, where 'bulk' represents the product of the bulk fluid density and the pore volume of the sorbent (*i.e.*, ρV_{pore}).

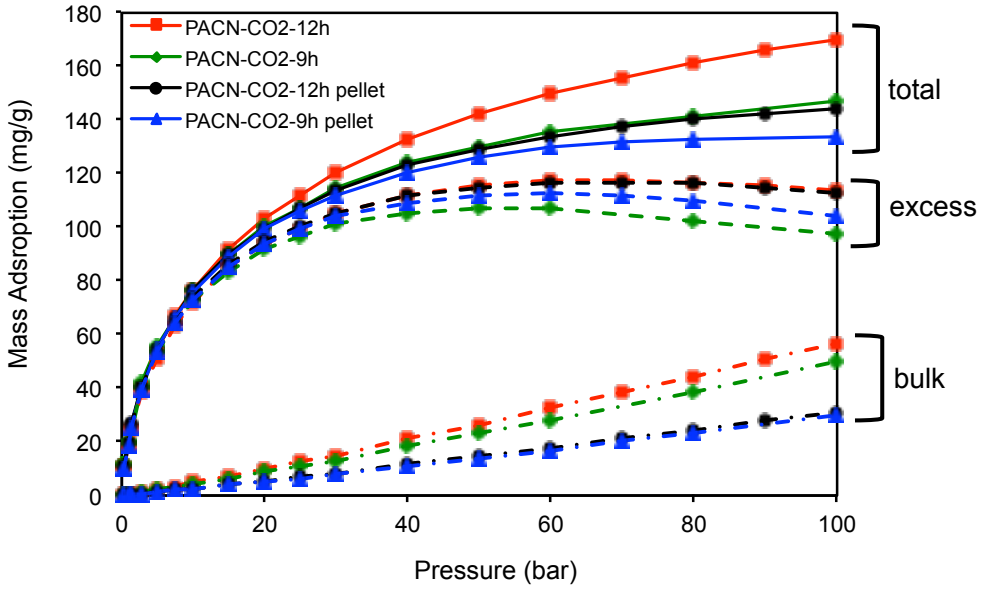

Figure S5. Comparison of total and excess adsorption of CH_4 at 298 K for the PACN materials.

Gravimetric and Volumetric Adsorption

The gravimetric adsorption can be converted into volumetric adsorption using the following equation.

$$n_{vol} = n_{grav} \frac{RT}{Mp} \rho_{s,bulk}$$

where n_{vol} is the volumetric adsorption in the unit of STP cc (of gas)/ cc (of sorbent), while n_{grav} is the gravimetric adsorption in the unit of mg (of gas)/ mg (of sorbent). R is the gas constant. M is the molecular mass of methane. T and p are the temperature and pressure at STP. $\rho_{s,bulk}$ represents the bulk density of the sorbent, which can be estimated from the following equation.

$$\rho_{s,bulk} = {m_s}/{(V_{true} + V_p)}$$

where m_s is the sorbent mass; V_{true} and V_p are the sorbent skeletal volume (i.e., true volume) and the pore volume, respectively. The sorbent mass and skeletal volume is obtained from the helium buoyancy measurements (Figure S3).

Isosteric Heat of Adsorption

The isosteric heat of adsorption (Q_{st}) was estimated for PACN-KOH and Maxsorb, using the methodology specified in a previous study.[5] The results are shown in the Figure S6. PACN-KOH shows higher Q_{st} than Maxsorb over the entire range of methane loadings measured. It can be noted that the Q_{st} for both materials decreases as the methane loading increases. At high methane loading (e.g., 15 mmol/g), the difference between the Q_{st} for the two materials becomes larger compared with low methane loading.

In a study by Li, et al., it was found that nitrogen sites in MOFs lead to enhanced methane storage capacity.[6] They also performed DFT studies which clearly showed that there exists an increase methane affinity for the nitrogen functional sites as Lewis base. They also found that the contribution of the nitrogen sites is more prominent at a higher pressure (e.g., 65 bar). This is consistent with the findings in Figure S6 that the PACN-KOH sample with nitrogen sites has stronger methane affinity compared with Maxsorb, and that the difference becomes more prominent at higher pressures.

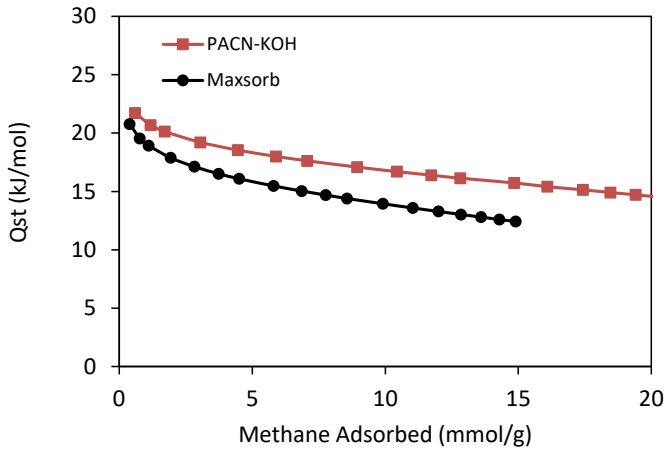

Figure S6. Isosteric heat of adsorption of methane onto PACN-KOH and Maxsorb as a function of methane loading.

Adsorption Data Validation

The N_2 sorption and CH_4 sorption isotherms for the commercial carbons, *i.e.*, CMK-3 and Maxsorb, obtained in this work are compared with the literature data. The comparison is shown in Figure S7. Note that the nitrogen sorption data for Maxsorb (Figure S7a) from this work matches well with two other papers in the literature, which verifies the accuracy of our nitrogen measurements. The CMK-3 samples (Figure S7b) varies to a certain degree across different papers, probably due to the samples from different vendors, variation in the synthetic procedures and/or different batches of synthesis, since the synthesis involves a number of variables including the mesoporous silica template, the carbon precursor, etc. In addition, the methane adsorption data obtained for Maxsorb (Figure S7c) in this work matches well with the literature results, which validates our methane adsorption measurements. The methane adsorption for CMK-3 (Figure S7d) in this work is in reasonable agreement with that in the literature. Interestingly, the methane adsorption in this work is slightly low than that from the literature at relatively low

pressure (< 25 bar), but is higher at relatively high pressure (> 25 bar). This is likely due to the slight difference in the pore structures of the CMK-3 used in our work and that in the literature, as indicated in the nitrogen sorption data at 77 K (Figure S7b).

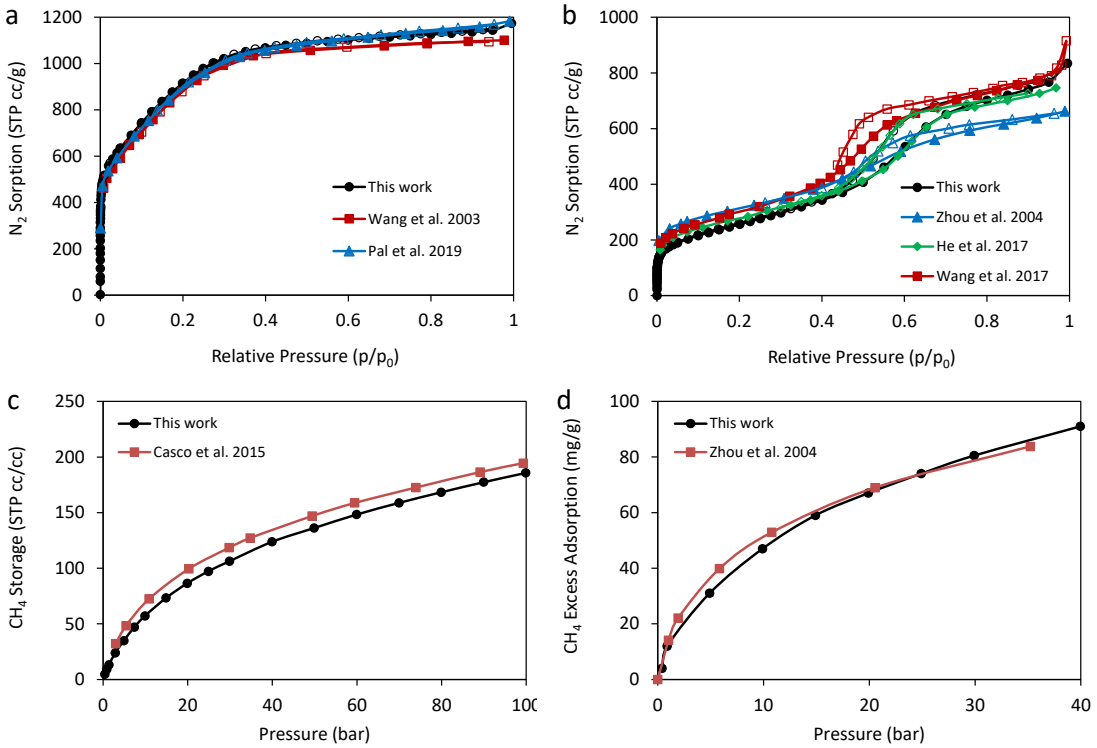

Figure S7. Comparison of data obtained in this work with those from the literature: Nitrogen sorption isotherms at 77 K of (a) maxsorb and (b) CMK-3; Methane adsorption isotherms at 298 K of (c) maxsorb and (d) CMK-3. [2,7-11]

Effect of the Sample Size in the Methane Adsorption Measurements

The minimum required amount of the sample varies depending on several factors, including the measurement technique (gravimetric vs. volumetric), the instrument's resolution, the sample's adsorption capacity, etc. In this work, we used a Rubotherm Magnetic Suspension Balance IsoSORB system with a resolution of 1 μg and a reproducibility of 2 μg. The methane storage measurements were corrected for dead volume using the skeletal volume of the sample measured by helium buoyancy. The

typical sample size in this study is around 200 mg. With methane capacity on the level of > 10 mg/g, the weight change caused by methane adsorption is > 2 mg (compared with a non-adsorbing sample under the same influence of gas buoyancy), which is much higher than the instrument detection limit. We have studied the impact of sample size (Figure S8). The results show that 100 mg was sufficient for our instrument.

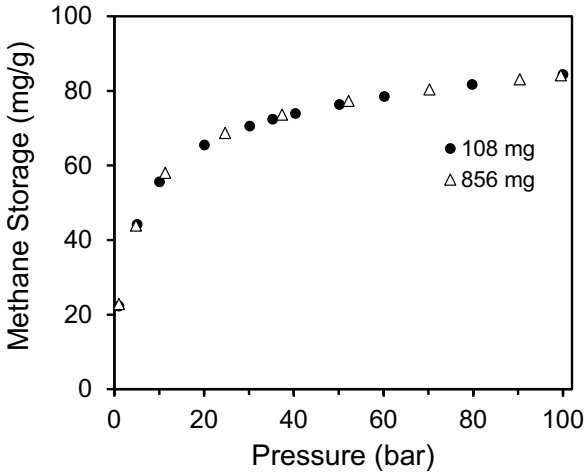

Figure S8. Methane storage data (25 ºC) of zeolite 13X pellets with different sample sizes.

References

(1) Tian, T.; Zeng, Z.; Vulpe, D.; Casco, M. E.; Divitini, G.; Midgley, P. A.; Silvestre-Albero, J.; Tan, J.-C.; Moghadam, P. Z.; Fairen-Jimenez, D. A sol–gel monolithic metal–organic framework with enhanced methane uptake. *Nature materials* **2018,** *17* (2), 174.

(2) Casco, M. E.; Martínez-Escandell, M.; Gadea-Ramos, E.; Kaneko, K.; Silvestre-Albero, J.; Rodríguez-Reinoso, F. High-pressure methane storage in porous materials: are carbon materials in the pole position? *Chemistry of Materials* **2015,** *27* (3), 959.

(3) Mason, J. A.; Veenstra, M.; Long, J. R. Evaluating metal–organic frameworks for natural gas storage. *Chemical Science* **2014,** *5* (1), 32.

(4) Lowell, S.; Shields, J. E.; Thomas, M. A.; Thommes, M. *Characterization of porous solids and powders: surface area, pore size and density*; Springer Science & Business Media, 2012.

(5) Whittaker, P. B.; Wang, X.; Regenauer-Lieb, K.; Chua, H. T. Predicting isosteric heats for gas adsorption. *Physical Chemistry Chemical Physics* **2013,** *15* (2), 473.

(6) Li, B.; Wen, H.-M.; Wang, H.; Wu, H.; Yildirim, T.; Zhou, W.; Chen, B. Porous metal–organic frameworks with Lewis basic nitrogen sites for high-capacity methane storage. *Energy & Environmental Science* **2015,** *8* (8), 2504.

(7) Wang, L.; Yang, R. T.; Sun, C. L. Graphene and other carbon sorbents for selective adsorption of thiophene from liquid fuel. *AIChE Journal* **2013,** *59* (1), 29.

(8) Pal, A.; Uddin, K.; Thu, K.; Saha, B. B. Activated carbon and graphene nanoplatelets based novel composite for performance enhancement of adsorption cooling cycle. *Energy Conversion and Management* **2019,** *180*, 134.

(9) Zhou, H.; Zhu, S.; Honma, I.; Seki, K. Methane gas storage in self-ordered mesoporous carbon (CMK-3). *Chemical Physics Letters* **2004,** *396* (4-6), 252.

(10) He, Z.; Zhang, G.; Chen, Y.; Xie, Y.; Zhu, T.; Guo, H.; Chen, Y. The effect of activation methods on the electrochemical performance of ordered mesoporous carbon for supercapacitor applications. *Journal of Materials Science* **2017,** *52* (5), 2422.

(11) Wang, L.; Zhao, H.; Zhang, D.; Song, W.; Xu, S.; Liu, S.; Li, Z. Ordered mesoporous carbon-supported CoFe 2 O 4 composite with enhanced lithium storage properties. *Journal of Materials Science* **2017,** *52* (11), 6265.